TITLE

The ZMYND8 chromatin factor protects cardiomyocyte identity and function in the mouse heart

AUTHORS

Andrew Kekūpaʻa Knutson, Abigail Avelar, and Ralph V. Shohet*

*Corresponding Author

AFFILIATIONS

Center for Cardiovascular Research, John A. Burns School of Medicine, University of Hawaiʻi, Honolulu, HI 96813

ABSTRACT

Appropriate gene expression within cardiomyocytes is coordinated by chromatin factors and is essential for heart function. We investigated the role of the chromatin reader ZMYND8 in the mouse heart using null and conditional knockouts (*Zmynd8-cKO)*. While full-length *Zmynd8* is not required for cardiomyocyte development, *Zmynd8-cKO* mice develop cardiomegaly, decreased cardiac function, and premature death compared to controls. Transcriptome analysis of *Zmynd8-cKO* cardiomyocytes reveals illegitimate expression of transcripts normally limited to skeletal muscle. Additionally, we observe integration of TNNI2 skeletal troponin into cardiac sarcomeres of mutant mice. We conclude that ZMYND8 is necessary to maintain appropriate cardiomyocyte homeostasis and gene expression.

INTRODUCTION

Cardiomyocytes are highly specialized, energy-demanding cells that produce contraction of the cardiac chambers. These cells are extremely sensitive to ATP depletion and are often the first to die under conditions of hypoxia (Knutson et al. 2021). Because adult cardiomyocytes cannot replicate, protecting these cells is a crucial goal of modern cardiovascular science. Defining the genetic factors and mechanisms that protect the cardiomyocyte gene program can potentially improve treatments for both congenital and acquired heart disease (Kathiresan and Srivastava 2012).

Transcriptional regulatory mechanisms are often dysregulated in cancer, neurological and cardiovascular diseases, leading to altered cellular function. The role that chromatin regulators play in coordinating cardiomyocyte development and the progression of heart disease is becoming increasingly apparent (Greco and Condorelli 2015). These factors can regulate transcription through different mechanisms including deposition of covalent histone marks associated with active or repressive gene expression, recruitment of transcriptional machinery, or enhancer and suppressor activity. A group of chromatin proteins that contain bromodomain motifs have recently attracted

attention as critical regulators of the progression of illness (Fujisawa and Filippakopoulos 2017). The transcriptional circuitry dysregulated in heart failure is of particular clinical importance.

ZMYND8 (also known as PRKCBP1 or RACK7) was initially characterized as a binding partner of Protein Kinase C in humans (Fossey et al. 2000) and has since been studied for its role in regulating gene expression, enhancer activity, and the DNA damage response (Shen et al. 2016; Spruijt et al. 2016). While ZMYND8 is not predicted to have enzymatic activity, it can recognize covalent modifications on histone tails including H3K4me1 and H3K14ac (and potentially other marks) through its PHD, Bromo, and PWWP domains (Li et al. 2016; Savitsky et al. 2016). An MYND domain recruits several chromatin writers and erasers to modulate the chromatin landscape. Although the role of ZMYND8 in the heart is unknown, mutations have been found in GWAS studies of nonsyndromic ventricular septal defects and other congenital cardiac abnormalities (Al Turki et al. 2014; Dias et al. 2022). Our lab has identified a role for ZMYND8 in suppressing the activity of hypoxia inducible factor, HIF-1, in a transgenic mouse model that expresses oxygen-stabilized HIF-1a in mouse cardiomyocytes (Schunke et al. 2019). Interestingly, acetylated ZMYND8 has been reported to have both activating and repressive roles in HIF-regulated gene expression in human breast cancers (Chen et al. 2018). These observations prompted us to investigate the role of ZMYND8 in mammalian cardiomyocytes.

Here, we describe physiological, cellular, and molecular consequences of removing full-length ZMYND8 from mouse cardiomyocytes. We find that while ZMYND8 is necessary for embryonic development, it is not necessary for cardiomyocyte development using two established Cre recombinase lines. However, adult mice lacking full-length ZMYND8 in their cardiomyocytes develop enlarged hearts, reduced cardiac function, and distorted cardiomyocyte shape compared to control mice. These mice have a shortened lifespan compared to control mice, with a larger effect in female animals. We also show that in young adult hearts ZMYND8 is necessary to repress specific genes, some of which are normally restricted to skeletal muscle. These data provide first evidence of a

mouse model of *Zmynd8*-related cardiomyopathy and reveal roles for ZMYND8 in maintaining cardiac homeostasis.

RESULTS AND DISCUSSION

Zmynd8 is essential for embryogenesis but dispensable for cardiac development

ZMYND8 belongs to a large family of bromodomain-containing proteins that regulate chromatin and gene expression (Fujisawa and Filippakopoulos 2017). These factors have cell-type-specific functions and are important in normal development and the progression of disease. The role of ZMYND8 in the heart is unknown. To test the necessity for ZMYND8 in the heart, we first performed crosses using null and conditional alleles of *Zmynd8* (Figure 1). The flox sites for the *Zmynd8*^{fl} allele (Delgado-Benito et al. 2018) span exon 4 of *Zmynd8,* which encodes amino acids 34-85 of the full-length protein (Figure 1). These amino acids encode the entire bipartite nuclear localization sequence for ZMYND8. Using this allele with *Myh6-Cre*, we isolated a recombined delta allele of *Zmynd8* (i.e., *Zmynd8*$^{\Delta}$) that could be inherited through the germline of heterozygous mice, thus affecting all cells of the embryo (see Materials and Methods section). No *Zmynd8*$^{\Delta/\Delta}$ mice were born from crosses of *Zmynd8*$^{\Delta/+}$ heterozygous mice (Figure 1B).

To understand the requirement for ZMYND8 specifically within the cardiomyocyte lineage, we used two Cre recombinase lines, *Myh6-Cre* (Agah et al. 1997) and *Nkx2.5-Cre* (Stanley et al. 2002), in combination with the *Zmynd8*^{fl} allele. Progeny from crosses of *Myh6-Cre*$^{Tg/0}$*; Zmynd8*$^{fl/+}$ males and *Zmynd8*$^{fl/fl}$ females were born at expected Mendelian ratios and survived to adulthood (Figure 1B). We repeated these crosses with *Nkx2.5-Cre*, which is active in cardiac precursors as early as E7.5 but may also induce recombination in the proepicardium and derivative cell types. Using the *Nkx2.5-Cre* line, we also observed progeny born at expected Mendelian ratios (Supplemental Fig. S1A).

We detected efficient flox recombination in heart tissue (Supplemental Fig. S1B) and differences in ZMYND8 protein sizes in *Zmynd8-cKO* heart tissue compared to control tissue using a

monoclonal ZMYND8 antibody (Supplemental Fig. S1C). We noticed that the observed proteins using this antibody in both control and *Zmynd8-cKO* heart tissue was approximately 30 kD lower than the predicted size of full-length ZMYND8. Compared to control hearts, a larger ~115 kD band is depleted and a shorter ~110 kD band becomes enriched in *Zmynd8-cKO* hearts. One explanation for this is that shorter isoforms of ZMYND8 exist in the heart and become preferentially expressed in this model. Consistent with this, immunoblots with a ZMYND8 polyclonal antibody resulted in several shorter proteins ranging in size from ~40 to 130 kilodaltons and could be detected in both control and *Zmynd8-cKO* hearts (Supplemental Fig. S1C). Full-length ZMYND8 could be detected with this polyclonal antibody from isolated spleens, which contain B cells that are known to express full-length ZMYND8 (Delgado-Benito et al. 2018). Another possibility is that proteolytic cleavage of ZMYND8 occurs using our cardiomyocyte or protein isolation methods and removal of exon 4 exposes a proteolytic site that is othewise protected. Indeed, ZMYND8 does contain an intrinsically disordered region, which contributes to its ability to aggregate and form liquid condensates at super enhancers (Jia et al. 2021).

To confirm that ZMYND8 was being depleted in cardiomyocytes, especially from nuclei, we performed ZMYND8 immunostaining of isolated cardiomyocytes and observed a reduction in ZMYND8 nuclear staining compared to control cardiomyocytes (Figure 1C and Supplemental Fig. S1D). Interestingly, we sometimes observed strong perinuclear localization in addition to nuclear staining of ZMYND8 in control cardiomyocytes. Perinuclear localization of ZMYND8 was only observed in a fraction of wild-type cardiomyocytes and certain binuclear cardiomyocytes had only one nucleus with perinuclear ZMYND8. ZMYND8 has been reported to have both nuclear and cytoplasmic localization in other cell types, including neurons, and its location is regulated by Drebrin (Yao et al. 2017). These results suggest that while full-length *Zmynd8* is necessary for embryonic development, it is not necessary for cardiomyocyte development, using the Cre lines we tested.

Knockout of *Zmynd8* in cardiomyocytes leads to cardiac dysfunction and death

While *Myh6-Cre*$^{Tg/0}$*; Zmynd8*$^{fl/fl}$ mice appeared normal during early adulthood, these mice had a reduced lifespan compared to *Myh6-Cre*$^{Tg/0}$ controls with most dying between 5 and 6 months of age (Figure 2A). Signs of distress prior to death included lethargy, tachypnea, a hunched back, and retention of fluid. Interestingly, there was a difference between male and female mortality with female *Zmynd8-cKO* mice having a slightly shorter lifespan than males (Supplemental Fig. 2). This contrasts with *Myh6-Cre*$^{Tg/0}$ control mice where no difference in lifespan between the sexes was detected (Supplemental Fig. 2). Heterozygous mice also showed a sex difference in lifespan with *Myh6-Cre*$^{Tg/0}$*; Zmynd8*$^{fl/+}$ females having a shorter lifespan than males (Supplemental Fig. 2). Additionally, in analyzing male and female *Myh6-Cre*$^{Tg/0}$*; Zmynd8*$^{fl/fl}$ siblings born in the same litter, female *Myh6-Cre*$^{Tg/0}$*; Zmynd8*$^{fl/fl}$ mice always died before their male siblings. ZMYND8 interacts with the X-linked demethylase KDM5C (Shen et al. 2016) and its Y-linked counterpart KDM5D (Li et al. 2016), raising the possibility that male and female *Zmynd8*-deficient cardiomyocytes could manifest sexually-dimorphic responses during heart failure. KDM5C and KDM5D are thought to be redundant in preventing a compact myocardium phenotype during embryogenesis (Kosugi et al. 2020), however no study has characterized deficiency of these enzymes isolated to the cardiomyocyte lineage.

We assessed heart morphology and function in *Zmynd8-cKO* mice and detected an increase in heart weight to body weight ratio as early as 6 weeks compared to sibling controls in both males and females (Figure 2B and 2C, Supplemental Fig. 2D). This heart enlargement progresses over time, with 5-month-old *Myh6-Cre*$^{Tg/0}$*; Zmynd8*$^{fl/fl}$ mice presenting an increase of 80% in heart mass compared to age-matched control mice (Figure 2B). Cross sections of 8-week-old *Myh6-Cre*$^{Tg/0}$*; Zmynd8*$^{fl/fl}$ mice showed thinning of the ventricular walls suggesting cardiac remodeling (Figure 2C). We assessed heart function in *Zmynd8-cKO* adult mice using echocardiography and observed a dramatic decrease in both ejection fraction and fractional shortening over time compared to *Myh6-Cre*$^{Tg/0}$ control mice (Figure 2D). Taken together, these results show that ZMYND8 is necessary to prevent the onset of contractile dysfunction that leads to heart failure and death.

***Zmynd8-cKO* cardiomyocytes misexpress skeletal muscle transcripts**

In addition to its role in regulating enhancer activity (Shen et al. 2016) and DNA damage (Spruijt et al. 2016), ZMYND8 is known to have repressive functions on transcription through the recruitment of other chromatin factors, namely members of the Nucleosome Remodeling and Deacetylase (NuRD) complex, EZH2 (part of Polycomb Repressive Complex 2), and lysine demethylases. To understand the effects of removing *Zmynd8* on cardiomyocyte gene expression, we performed transcriptome analysis of cardiomyocytes isolated from control (i.e., *Myh6-Cre*$^{Tg/0}$) and *Zmynd8-cKO* (i.e., *Myh6-Cre*$^{Tg/0}$*; Zmynd8*$^{fl/fl}$) mice (Figure 3A). We assayed young (i.e., 4-week old adults) to capture the primary effects of *Zmynd8* knockout to avoid secondary transcriptional effects that could correlate with heart failure (Figure 2D). We confirmed that our cardiomyocyte isolation procedure produced pure populations of rod cardiomyocytes.

As expected, reads mapping to exon 4 of *Zmynd8* were detected in control samples but were substantially reduced in *Zmynd8-cKO* cardiomyocytes, suggesting both a high degree of cardiomyocyte purity and efficient recombination of the flox sites (Supplemental Fig. 3A). However, we did observe reads mapping to later exons of *Zmynd8* in *Zmynd8-cKO* cardiomyocytes, suggesting that nonsense-mediated decay may not be removing all *Zmynd8* transcripts in these cells. Interestingly, levels of reads mapping to the later exons of *Zmynd8* appeared to increase upon Cre recombination. This result is consistent with immunoblots that show enrichment of a shorter band in *Zmynd8-cKO* animal hearts (Supplemental Fig. 1C), however further characterization of potential mRNA and protein isoforms is needed. Regulation of the *Zmynd8* transcript, perhaps through changes in mRNA splicing, or autoregulation of the *Zmynd8* locus by ZMYND8 and its associated machinery may be possible explanations for these observations.

We observed subtle changes in gene expression from young cardiomyocytes. Using a cutoff of 1.5-fold in either direction and an adjusted p-value of less than 0.05, we observed 55 genes upregulated and 4 genes downregulated in 4-week post-partum *Zmynd8-cKO* cardiomyocytes (Figure

3B). Gene ontology analysis of the 55 upregulated genes produced categories of striated muscle contraction including cardiac muscle and skeletal muscle and genes related to cation transport (Figure 3C and 3D). Compared to control cardiomyocytes, certain genes normally expressed only in skeletal muscle are abundant in *Zmynd8-cKO* cardiomyocytes including those encoding the fast-twitch troponin *Tnni2*, the calcium sensor *Casq1*, and the skeletal muscle myosin *Myl1* (Figure 3C and Supplemental Fig. 3). Cardiomyocytes expressing skeletal muscle contractile genes have been observed in embryonic mouse hearts deficient in NuRD complex components including *Hdac1/2* (Montgomery et al. 2007), *Chd4* (Gomez-Del Arco et al. 2016; Wilczewski et al. 2018) as well as adult hearts lacking *Ezh2* (Delgado-Olguin et al. 2012). ZMYND8 has been shown to interact with the NuRD subunit GATAD2 (Spruijt et al. 2016), as well as phosphorylated EZH2 (Tang et al. 2021) although these studies were not performed in the heart. Additionally, CHD4 has recently been shown to be recruited by GATA4 and NKX-2.5 to specific loci to repress gene expression programs in embryonic cardiomyocytes (Robbe et al. 2022); it is unknown if ZMYND8 is also involved in this process. While one hypothesis is that ZMYND8 is an additional factor, like GATA4 or NKX-2.5, that recruits CHD4 to specific gene promoters, another hypothesis is that ZMYND8 regulates the accessibility or function of enhancers associated with these genes. In addition to *Chd4, Ezh2*, and now *Zmynd8* mutants, illegitimate expression of skeletal genes in cardiomyocytes has also been observed in mice lacking *Prox1* (Petchey et al. 2014), *Ctcf* (Gomez-Velazquez et al. 2017), the RNA-binding protein TRBP (Ding et al. 2015), or the H3.3 histone chaperone HIRA (Dilg et al. 2016). Defining how these factors work in concert to normally repress skeletal muscle gene expression in cardiomyocytes should be a focus of future work.

Although there were only 4 downregulated genes in *Zmynd8-cKO* cardiomyocytes compared to control they include the cardiomyocyte transcription factor *Hopx* and the cardiac myosin light chain gene *Myl9* (Figure 1C and Supplemental Fig. S3C). HOPX is a homeodomain protein that has been shown to direct cardiomyoblast formation but has not been extensively studied in adult cardiomyocytes (Jain et al. 2015). Based on these data, we conclude that ZMYND8 influences

expression of a limited number of important genes in cardiomyocytes. Correct expression or repression of these genes in cardiomyocytes may be necessary for proper cardiomyocyte function.

ZMYND8 regulates cardiac sarcomere formation and cardiomyocyte morphology

Cardiomyocyte sarcomeres rely on appropriate stoichiometry of their components to generate the necessary contractile force that sustain heart beats. Deficiencies in sarcomere structure can lead to a range of cardiomyopathies (Lehman et al. 2022). Cardiac and skeletal versions of troponins have different calcium handling properties and integration of skeletal troponin can affect cardiac sarcomere contraction when expressed in cardiomyocytes (Wilczewski et al. 2018). To determine if transcripts encoding skeletal muscle troponin are translated into protein and incorporated into sarcomeres in *Zmynd8-cKO* cardiomyocytes, we performed immunohistochemistry for the cardiac M-band protein MYOM1 and the skeletal troponin TNNI2 on isolated *Zmynd8-cKO* cardiomyocytes. We observed robust TNNI2 integration into cardiac sarcomeres in conditional knockout mice using either *Myh6-Cre* or *Nkx2.5-Cre* (Figure 3A and Supplemental Fig. S4). Interestingly, only a fraction of cardiomyocytes from each knockout model misexpressed TNNI2 (Supplemental Fig. S4).

Upon isolating ventricular cardiomyocytes from *Zmynd8-cKO* mice, we observed a subset of cardiomyocytes had a distorted shape compared to control. We measured cardiomyocyte area, length, and width and found that some cardiomyocytes isolated from the *Zmynd8-cKO* hearts were shorter and broader than control cells (Figure 4B). We did not observe a correlation between TNNI2 expression and cardiomyocyte shape (Supplemental Fig. S4) suggesting distorted cardiomyocyte morphology is a result of other mechanisms independent of TNNI2 integration into sarcomeres. Taken together, these data show that ZMYND8 regulates the proper formation of cardiac sarcomeres as well as cardiomyocyte morphology in the mouse heart.

Our study examines the role of ZMYND8 in mouse cardiomyocytes and we believe this work sheds light on the function of this protein in human genetic disease. Mutations in *Zmynd8* have been found in patients with both neurocognitive and congenital heart defects (Al Turki et al. 2014; Dias et

al. 2022). Understanding the mechanism in which ZMYND8 works to prevent the onset of cardiac dysfunction will be a focus of future work. ZMYND8 could be working, through recruitment of associated chromatin factors (e.g. NuRD complex), by repressing gene expression at promoter regions (Figure 4C). Alternatively, ZMYND8 could prevent the activation of enhancer elements upstream of these genes (Figure 4C). Upon depletion of ZMYND8 from cardiomyocytes, enhancer-promoter interactions at these genes are allowed to form via other transcription factors, leading to gene expression and the phenotypes we report in this study (Figure 4C).

Although we are confident that ZMYND8 is depleted from cardiomyocyte nuclei in our model, deeper analysis of the functions of the shorter *Zmynd8* isoforms in the heart could reveal additional insights. Also, given that ZMYND8 is reported to interact with several chromatin factors (including KDM5C and KDM5D) in other cell types, delineating which factors are working with ZMYND8 in cardiomyocytes should be done. Finally, while our experiments correlate ZMYND8's gene repressive activities and cardiac function, we cannot rule out that the observed physiological phenotypes relate to other reported functions of ZMYND8 including its role in the DNA damage pathway. Indeed, the inability to resolve DNA damage in cardiomyocytes has recently been shown to contribute to cardiomyopathy progression (Higo et al. 2017). Taken together, our results provide evidence that ZMYND8 is an important chromatin regulator of cardiomyocyte gene expression and function.

MATERIALS AND METHODS

Mouse Strains and Husbandry

Zmynd8^{fl} mice were generously provided by Dr. Michela Di Virgilo and described previously (Delgado-Benito et al. 2018). This mouse was backcrossed onto a C57BL/6 background for 10 generations before being used in experiments. *Myh6-Cre* (Agah et al. 1997) and *Nkx2.5*-Cre (Stanley et al. 2002) mice were obtained from Jackson Labs and were backcrossed to C57BL/6 for at least 5 generations before being used in experiments. Mice were maintained in standard conditions with normal chow *ad libitum*. All protocols were approved by the University of Hawai'i IACUC. Primers

used for genotyping the *Zmynd8*^{fl} allele are Primer Prkcbp1_35576_5 5'-GACCACAGCTCTTGCACAGG-3', Primer ZMYND8_R2(Rev) 5'-AAGAAAACCCTGAGACCACC-3', and Primer MDV_p240 5'-GTGCAAACGTGTTCAGTGG-3'(Delgado-Benito et al. 2018) . Primers used to genotype both *Myh6-Cre* and *Nk2.5-Cre* lines are Primer Cre_F 5'-TCCAATTTACTGACCGTACACCAA-3' and Primer Cre_R 5'-CCTGATCCTGGCAATTTCGGCTA-3'.

To generate *Zmynd8-cKO* mice, *Myh6-Cre*$^{Tg/0}$*; Zmynd8*$^{fl/+}$ or *Nkx2.5-Cre*$^{Tg/0}$*; Zmynd8*$^{fl/+}$ males were bred with *Zmynd8*$^{fl/fl}$ females. The *Myh6-Cre* transgene, when inherited through the mother, induces recombination in approximately ~1% of germ cells (Eckardt et al. 2004). Using this knowledge, we isolated the recombined allele of *Zmynd8* (i.e., *Zmynd8*$^{\Delta}$*)* that could be propagated in heterozygotes and confirmed using the *Zmynd8*^{fl} primers listed above.

Echochardiography

Heart function was assessed on unsedated animals using a 32 MHz transducer with a Vevo 2011 system (VisualSonics) as described previously (Williams et al. 2018). Both data collection and analysis were blinded for genotype.

Cardiomyocyte Isolation

Cardiomyocyte isolation from adult mice were performed using a Langedorff-free method described previously, with minor modifications (Ackers-Johnson et al. 2016). Briefly, after deep anesthesia, the chest was opened and hearts were excised, blood was removed by perfusion and the heart was digested with collagenases 2 and 4 (Worthington) and Protease XIV (Sigma). All buffers were supplemented with 25 nM Blebbistatin (Toronto Chemicals) to inhibit contraction. The atria and great vessels were removed, and ventricular heart tissue was manually dissociated followed by a brief, gentle 2-minute trituration with a pipette. The resulting cell suspension was filtered through a 100 μm strainer to remove large pieces of tissue. Cardiomyocytes were enriched during gravity settlement steps with gradually introduced Ca^{2+}, followed by plating on laminin-coated dishes or

coverslips to remove rounded cardiomyocytes and other cell types (e.g., fibroblasts, endothelial cells, blood cells).

Immunostaining and Microscopy Analysis

Isolated cardiomyocytes were plated onto coverslips and then fixed in 4% paraformaldehyde for 10 minutes at 37 ^{o}C, followed by three washes of PBS at room temperature. Cells were blocked and permeabilized using a PermBlock solution (2% FBS, 2% BSA, and 0.1% IGEPAL CA-630 in PBS) and then incubated with primary antibodies diluted in PermBlock solution overnight at 4 ^{o}C. Antibodies used in this study include anti-MYOM1 (Developmental Studies Hybridoma Bank), anti-ZMYND8 (Sigma HPA020949), and anti-TNNI2 (Proteintech 11634-1-AP). Cells were washed and then incubated with secondary antibodies conjugated with either Alexa Fluor 488 or 594 (ThermoFisher), washed again in PBS-Tween and then sealed with Prolong mountant with DAPI. Images were obtained on a Leica SP5 Confocal Microscope with control and experimental images taken at the same laser intensity and exposure. Images were processed using ImageJ and control and experimental images treated identically. To assess nuclear intensity of ZMYND8 in control and *Zmynd8-cKO* cardiomyocytes, we used the polyclonal anti-ZMYND8 antibody. Briefly, single plane slices of nuclei were imaged and regions of interests (ROI) were determined manually in ImageJ using the DAPI channel. These ROI's were overlayed onto the ZMYND8 channel and pixel intensities were recorded. To account for background staining, normalization ROIs were defined just adjacent to each nucleus (i.e, in the cytoplasmic region) and subtracted from its corresponding nucleus. We made sure not to include any perinuclear ZMYND8 staining in our analyses. The corrected mean nuclear intensities were then plotted and an unpaired t-test was performed to determine significance.

Immunoblotting

Immunoblotting of heart tissue has been described previously (Williams et al. 2018). Briefly, heart tissue left over from cardiomyocyte isolations was pulverized in liquid nitrogen and extracted in

RIPA Buffer with protease inhibitors (Roche). Blots were incubated with anti-ZMYND8 monocolonal (Abcam ab201452) or anti-ZMYND8 polyclonal (Sigma HPA020949) antibodies overnight. The next day, blots were washed in PBS + 0.2% Tween-20 and then incubated with fluorescent-conjugated IRDye secondary antibodies (LiCOR). Blots were imaged on a LiCOR Odyssey IR Imaging System.

RNA-seq and Analysis

Total RNA from isolated cardiomyocytes was extracted in Trizol and RNA quality was assessed on a Bioanalyzer. Only RNA with an RNA Integrity Number of >7 was used in library construction. Approximately 250 ng of RNA was used to construct each library. Ribosomal RNA was depleted using NEBNext rRNA Depletion Kit original or v2 (Human/Mouse/Rat) (E6310 or E7400) and libraries were built using the NEBNext Ultra II RNA Library Prep Kit for Illumina (E7770). The libraries were multiplexed and sequenced on a NextSeq500 at 75 bp single-end reads.

Reads were aligned to the mm10 mouse genome using HISAT2 (Kim et al. 2019) and duplicate reads were excluded from analyses. Differential gene expression was determined using DESeq2 (Love et al. 2014) with default parameters. Subsequent analyses and plot generation was performed in R. Reads were converted to bam files and visualized using IGV. Gene ontology analysis was performed using DAVID software. RNA-seq data have been deposited in Gene Expression Omnibus under accession number GSEXXXX.

COMPETING INTEREST STATEMENT

No potential competing interests are reported by the authors.

ACKNOWLEDGEMENTS

We thank Dr. Michela Di Virgilio for kindly sharing the *Zmynd8*^{fl} mouse. We also thank Dr. Kathryn Schunke for discussions prior to this work being initiated. This work used the Genomics Shared Resource Core at the UH Cancer Center, which is funded by an NCI Cancer Center Support

Grant (P30CA071789), the JABSOM Histology Core, and the Mouse Phenotyping Core. Dr. Knutson has been supported by a Ruth R. Kirschstein Postdoctoral Fellowship (HL149319), a MOSAIC K99 (GM145410), a Burroughs Wellcome Fund Postdoctoral Enrichment Program Award, and a T32 training grant (HL115505).

A.K.K. and R.V.S designed the experiments. A.K.K. performed all experiments and analyses except for echocardiography experiments, which were performed and evaluated by A.A. A.K.K. and R.V.S. interpreted data and wrote the manuscript. All authors edited and approved the final manuscript.

FIGURE LEGENDS

Figure 1. ZMYND8 is necessary for embryonic development but is not required for cardiomyocyte development. **A)** Schematic of the *Zmynd8* gene with the wild-type (+), floxed (flox), and delta (Δ) alleles. **B)** Breeding strategy and mendelian ratios of *Zmynd8*$^{\Delta}$ crosses (left) and *Myh6-Cre*$^{Tg/0}$*; Zmynd8*$^{fl/fl}$ crosses (right). Expected (Exp) and observed (Obs) number of progeny and percentages are indicated for each cross. **C)** Immunofluoresence staining of control (*Myh6-Cre*$^{Tg/0}$) and *Zmynd8-cKO* cardiomyocytes for MYOM1 (red), ZMYND8 (green), and DNA (blue). The nuclei outlined in boxes are expanded to the right. Scale bars are 50 μm. Normalized ZMYND8 nuclear intensity comparisons between control and *Zmynd8-cKO* cardiomyocytes is to the right with statistical significance calculated using an unpaired t-test.

Figure 2. Mice lacking *Zmynd8* in cardiomyocytes die with enlarged hearts. **A)** Lifespan analysis of wild type (black circles), *Myh6-Cre*$^{Tg/0}$ (orange circles), *Myh6-Cre*$^{Tg/0}$*; Zmynd8*$^{fl/+}$ (red triangles); and *Myh6-Cre*$^{Tg/0}$*; Zmynd8*$^{fl/fl}$ (purple diamonds). Curve comparisons, p-values, and number of animals in each group can be found in Supplementary File 1. **B)** Heart weight to body weight ratios of 6-week old control and 6-week and 20-week old *Myh6-Cre*$^{Tg/0}$*; Zmynd8*$^{fl/fl}$ mice. **C)** Stereoscopic image of

whole hearts from 4-month-old control and *Zmynd8-cKO* male mice (top) and H&E staining of transverse sections (bottom). Arrowheads indicate papillary muscles. **D)** Ejection Fraction and Fractional Shortening measurements of *Myh6-Cre*$^{Tg/0}$ control (orange circles) and *Myh6-Cre*$^{Tg/0}$*; Zmynd8*$^{fl/fl}$ (purple diamonds) adult mice over time. Each point is an individual mouse with best-fit curves calculated using non-linear regression.

Figure 3. Gene expression changes in *Zmynd8-cKO* adult cardiomyocytes. **A)** Schematic of RNA-seq experiment. Cardiomyocytes were isolated from 4-week-old control (two females) and *Zmynd8-cKO* (two females and two males) mice and RNA was extracted, rRNA depleted, and sequenced. **B)** MA plot of genes up- and down-regulated in 4-week old *Zmynd8-cKO* female cardiomyocytes versus control female cardiomyocytes. Significant genes are colored purple and the number of up- or down-regulated genes are indicated. **C)** Heatmap of normalized $\log_2$(RPKM) values for each replicate. Genes are listed based on heatmap clustering. **D)** Gene ontology analysis of 55 upregulated genes using DAVID software.

Figure 4. *ZMYND8-cKO* cardiomyocytes integrate TNNI2 into their sarcomeres and have a distorted morphology. **A)** Confocal image of control and *Zmynd8-cKO* cardiomyocytes stained for MYOM1 (red), TNNI2 (green), and DNA (blue). Higher magnifications of boxed region are shown to the right. Scale bars are 50 µm. **C)** Morphometry data for cardiomyocytes isolated from two control (i.e., *Myh6-Cre*$^{Tg/0}$) and two *Zmynd8*-cKO adults. At least 75 cardiomyocytes were analyzed from each mouse. P-values are derived from unpaired t-tests. **C)** Models of ZMYND8 activity in cardiomyocytes. In ZMYND8(+) cardiomyocytes (left), ZMYND8 could be working at promoters and/or enhancers. In ZMYND8(-) cardiomyocytes (right), enhancer-promoter interactions occur via transcription factors (TFs), leading to expression of skeletal muscle genes, altered cardiomyocyte shape, and reduced cardiac function.

REFERENCES

Ackers-Johnson M, Li PY, Holmes AP, O'Brien SM, Pavlovic D, Foo RS. 2016. A Simplified, Langendorff-Free Method for Concomitant Isolation of Viable Cardiac Myocytes and Nonmyocytes From the Adult Mouse Heart. *Circ Res* **119**: 909-920.

Agah R, Frenkel PA, French BA, Michael LH, Overbeek PA, Schneider MD. 1997. Gene recombination in postmitotic cells. Targeted expression of Cre recombinase provokes cardiac-restricted, site-specific rearrangement in adult ventricular muscle in vivo. *J Clin Invest* **100**: 169-179.

Al Turki S, Manickaraj AK, Mercer CL, Gerety SS, Hitz MP, Lindsay S, D'Alessandro LC, Swaminathan GJ, Bentham J, Arndt AK et al. 2014. Rare variants in NR2F2 cause congenital heart defects in humans. *Am J Hum Genet* **94**: 574-585.

Chen Y, Zhang B, Bao L, Jin L, Yang M, Peng Y, Kumar A, Wang JE, Wang C, Zou X et al. 2018. ZMYND8 acetylation mediates HIF-dependent breast cancer progression and metastasis. *J Clin Invest* **128**: 1937-1955.

Delgado-Benito V, Rosen DB, Wang Q, Gazumyan A, Pai JA, Oliveira TY, Sundaravinayagam D, Zhang W, Andreani M, Keller L et al. 2018. The Chromatin Reader ZMYND8 Regulates Igh Enhancers to Promote Immunoglobulin Class Switch Recombination. *Mol Cell* **72**: 636-649 e638.

Delgado-Olguin P, Huang Y, Li X, Christodoulou D, Seidman CE, Seidman JG, Tarakhovsky A, Bruneau BG. 2012. Epigenetic repression of cardiac progenitor gene expression by Ezh2 is required for postnatal cardiac homeostasis. *Nat Genet* **44**: 343-347.

Dias KR, Carlston CM, Blok LER, De Hayr L, Nawaz U, Evans CA, Bayrak-Toydemir P, Htun S, Zhu Y, Ma A et al. 2022. De Novo ZMYND8 variants result in an autosomal dominant neurodevelopmental disorder with cardiac malformations. *Genet Med*.

Dilg D, Saleh RN, Phelps SE, Rose Y, Dupays L, Murphy C, Mohun T, Anderson RH, Scambler PJ, Chapgier AL. 2016. HIRA Is Required for Heart Development and Directly Regulates Tnni2 and Tnnt3. *PLoS One* **11**: e0161096.

Ding J, Chen J, Wang Y, Kataoka M, Ma L, Zhou P, Hu X, Lin Z, Nie M, Deng ZL et al. 2015. Trbp regulates heart function through microRNA-mediated Sox6 repression. *Nat Genet* **47**: 776-783.

Eckardt D, Theis M, Doring B, Speidel D, Willecke K, Ott T. 2004. Spontaneous ectopic recombination in cell-type-specific Cre mice removes loxP-flanked marker cassettes in vivo. *Genesis* **38**: 159-165.

Fossey SC, Kuroda S, Price JA, Pendleton JK, Freedman BI, Bowden DW. 2000. Identification and characterization of PRKCBP1, a candidate RACK-like protein. *Mamm Genome* **11**: 919-925.

Fujisawa T, Filippakopoulos P. 2017. Functions of bromodomain-containing proteins and their roles in homeostasis and cancer. *Nat Rev Mol Cell Biol* **18**: 246-262.

Gomez-Del Arco P, Perdiguero E, Yunes-Leites PS, Acin-Perez R, Zeini M, Garcia-Gomez A, Sreenivasan K, Jimenez-Alcazar M, Segales J, Lopez-Maderuelo D et al. 2016. The Chromatin Remodeling Complex Chd4/NuRD Controls Striated Muscle Identity and Metabolic Homeostasis. *Cell Metab* **23**: 881-892.

Gomez-Velazquez M, Badia-Careaga C, Lechuga-Vieco AV, Nieto-Arellano R, Tena JJ, Rollan I, Alvarez A, Torroja C, Caceres EF, Roy AR et al. 2017. CTCF counter-regulates cardiomyocyte development and maturation programs in the embryonic heart. *PLoS Genet* **13**: e1006985.

Greco CM, Condorelli G. 2015. Epigenetic modifications and noncoding RNAs in cardiac hypertrophy and failure. *Nat Rev Cardiol* **12**: 488-497.

Higo T, Naito AT, Sumida T, Shibamoto M, Okada K, Nomura S, Nakagawa A, Yamaguchi T, Sakai T, Hashimoto A et al. 2017. DNA single-strand break-induced DNA damage response causes heart failure. *Nat Commun* **8**: 15104.

Jain R, Li D, Gupta M, Manderfield LJ, Ifkovits JL, Wang Q, Liu F, Liu Y, Poleshko A, Padmanabhan A et al. 2015. HEART DEVELOPMENT. Integration of Bmp and Wnt signaling by Hopx specifies commitment of cardiomyoblasts. *Science* **348**: aaa6071.

Jia P, Li X, Wang X, Yao L, Xu Y, Hu Y, Xu W, He Z, Zhao Q, Deng Y et al. 2021. ZMYND8 mediated liquid condensates spatiotemporally decommission the latent super-enhancers during macrophage polarization. *Nat Commun* **12**: 6535.

Kathiresan S, Srivastava D. 2012. Genetics of human cardiovascular disease. *Cell* **148**: 1242-1257.

Kim D, Paggi JM, Park C, Bennett C, Salzberg SL. 2019. Graph-based genome alignment and genotyping with HISAT2 and HISAT-genotype. *Nat Biotechnol* **37**: 907-915.

Knutson AK, Williams AL, Boisvert WA, Shohet RV. 2021. HIF in the heart: development, metabolism, ischemia, and atherosclerosis. *J Clin Invest* **131**.

Kosugi M, Otani M, Kikkawa Y, Itakura Y, Sakai K, Ito T, Toyoda M, Sekita Y, Kimura T. 2020. Mutations of histone demethylase genes encoded by X and Y chromosomes, Kdm5c and Kdm5d, lead to noncompaction cardiomyopathy in mice. *Biochem Biophys Res Commun*.

Lehman SJ, Crocini C, Leinwand LA. 2022. Targeting the sarcomere in inherited cardiomyopathies. *Nat Rev Cardiol* **19**: 353-363.

Li N, Li Y, Lv J, Zheng X, Wen H, Shen H, Zhu G, Chen TY, Dhar SS, Kan PY et al. 2016. ZMYND8 Reads the Dual Histone Mark H3K4me1-H3K14ac to Antagonize the Expression of Metastasis-Linked Genes. *Mol Cell* **63**: 470-484.

Love MI, Huber W, Anders S. 2014. Moderated estimation of fold change and dispersion for RNA-seq data with DESeq2. *Genome Biol* **15**: 550.

Montgomery RL, Davis CA, Potthoff MJ, Haberland M, Fielitz J, Qi X, Hill JA, Richardson JA, Olson EN. 2007. Histone deacetylases 1 and 2 redundantly regulate cardiac morphogenesis, growth, and contractility. *Genes Dev* **21**: 1790-1802.

Petchey LK, Risebro CA, Vieira JM, Roberts T, Bryson JB, Greensmith L, Lythgoe MF, Riley PR. 2014. Loss of Prox1 in striated muscle causes slow to fast skeletal muscle fiber conversion and dilated cardiomyopathy. *Proc Natl Acad Sci U S A* **111**: 9515-9520.

Robbe ZL, Shi W, Wasson LK, Scialdone AP, Wilczewski CM, Sheng X, Hepperla AJ, Akerberg BN, Pu WT, Cristea IM et al. 2022. CHD4 is recruited by GATA4 and NKX2-5 to repress noncardiac gene programs in the developing heart. *Genes Dev* **36**: 468-482.

Savitsky P, Krojer T, Fujisawa T, Lambert JP, Picaud S, Wang CY, Shanle EK, Krajewski K, Friedrichsen H, Kanapin A et al. 2016. Multivalent Histone and DNA Engagement by a PHD/BRD/PWWP Triple Reader Cassette Recruits ZMYND8 to K14ac-Rich Chromatin. *Cell Rep* **17**: 2724-2737.

Schunke KJ, Walton CB, Veal DR, Mafnas CT, Anderson CD, Williams AL, Shohet RV. 2019. Protein kinase C binding protein 1 inhibits hypoxia-inducible factor-1 in the heart. *Cardiovasc Res* **115**: 1332-1342.

Shen H, Xu W, Guo R, Rong B, Gu L, Wang Z, He C, Zheng L, Hu X, Hu Z et al. 2016. Suppression of Enhancer Overactivation by a RACK7-Histone Demethylase Complex. *Cell* **165**: 331-342.

Spruijt CG, Luijsterburg MS, Menafra R, Lindeboom RG, Jansen PW, Edupuganti RR, Baltissen MP, Wiegant WW, Voelker-Albert MC, Matarese F et al. 2016. ZMYND8 Co-localizes with NuRD on Target Genes and Regulates Poly(ADP-Ribose)-Dependent Recruitment of GATAD2A/NuRD to Sites of DNA Damage. *Cell Rep* **17**: 783-798.

Stanley EG, Biben C, Elefanty A, Barnett L, Koentgen F, Robb L, Harvey RP. 2002. Efficient Cre-mediated deletion in cardiac progenitor cells conferred by a 3'UTR-ires-Cre allele of the homeobox gene Nkx2-5. *Int J Dev Biol* **46**: 431-439.

Tang B, Sun R, Wang D, Sheng H, Wei T, Wang L, Zhang J, Ho TH, Yang L, Wei Q et al. 2021. ZMYND8 preferentially binds phosphorylated EZH2 to promote a PRC2-dependent to -independent function switch in hypoxia-inducible factor-activated cancer. *Proc Natl Acad Sci U S A* **118**.

Wilczewski CM, Hepperla AJ, Shimbo T, Wasson L, Robbe ZL, Davis IJ, Wade PA, Conlon FL. 2018. CHD4 and the NuRD complex directly control cardiac sarcomere formation. *Proc Natl Acad Sci U S A* **115**: 6727-6732.

Williams AL, Khadka V, Tang M, Avelar A, Schunke KJ, Menor M, Shohet RV. 2018. HIF1 mediates a switch in pyruvate kinase isoforms after myocardial infarction. *Physiol Genomics* **50**: 479-494.

Yao N, Li J, Liu H, Wan J, Liu W, Zhang M. 2017. The Structure of the ZMYND8/Drebrin Complex Suggests a Cytoplasmic Sequestering Mechanism of ZMYND8 by Drebrin. *Structure* **25**: 1657-1666 e1653.

A

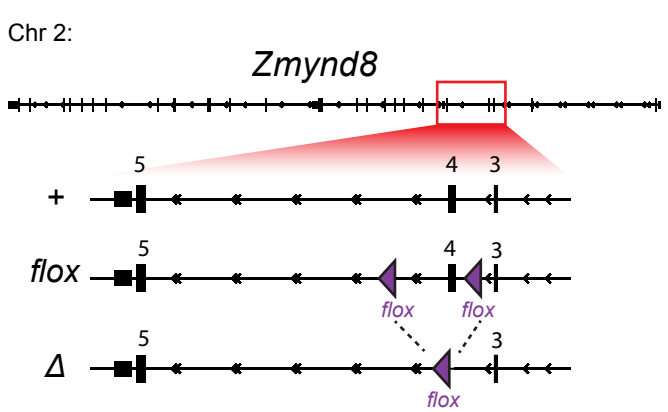

B

Zmynd8$^{\Delta/+}$ **x** *Zmynd8*$^{\Delta/+}$

Genotype	Exp (%)	Obs (%)
Zmynd8$^{+/+}$	5.75 (25)	5 (22)
Zmynd8$^{\Delta/+}$	11.5 (50)	18 (78)
Zmynd8$^{\Delta/\Delta}$	5.75 (25)	0 (0)

Myh6-Cre$^{Tg/0}$*; Zmynd8*$^{fl/+}$ **x** *Zmynd8*$^{fl/fl}$

Genotype	Exp (%)	Obs (%)
Zmynd8$^{fl/+}$	28.75 (25)	24 (21)
Zmynd8$^{fl/fl}$	28.75 (25)	31 (27)
Myh6-Cre$^{Tg/0}$*; Zmynd8*$^{fl/+}$	28.75 (25)	29 (25)
Myh6-Cre$^{Tg/0}$*; Zmynd8*$^{fl/fl}$	28.75 (25)	31 (27)

C

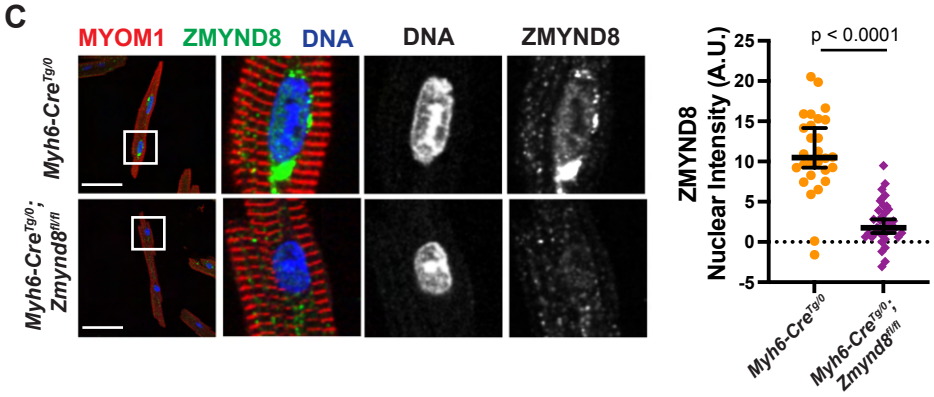

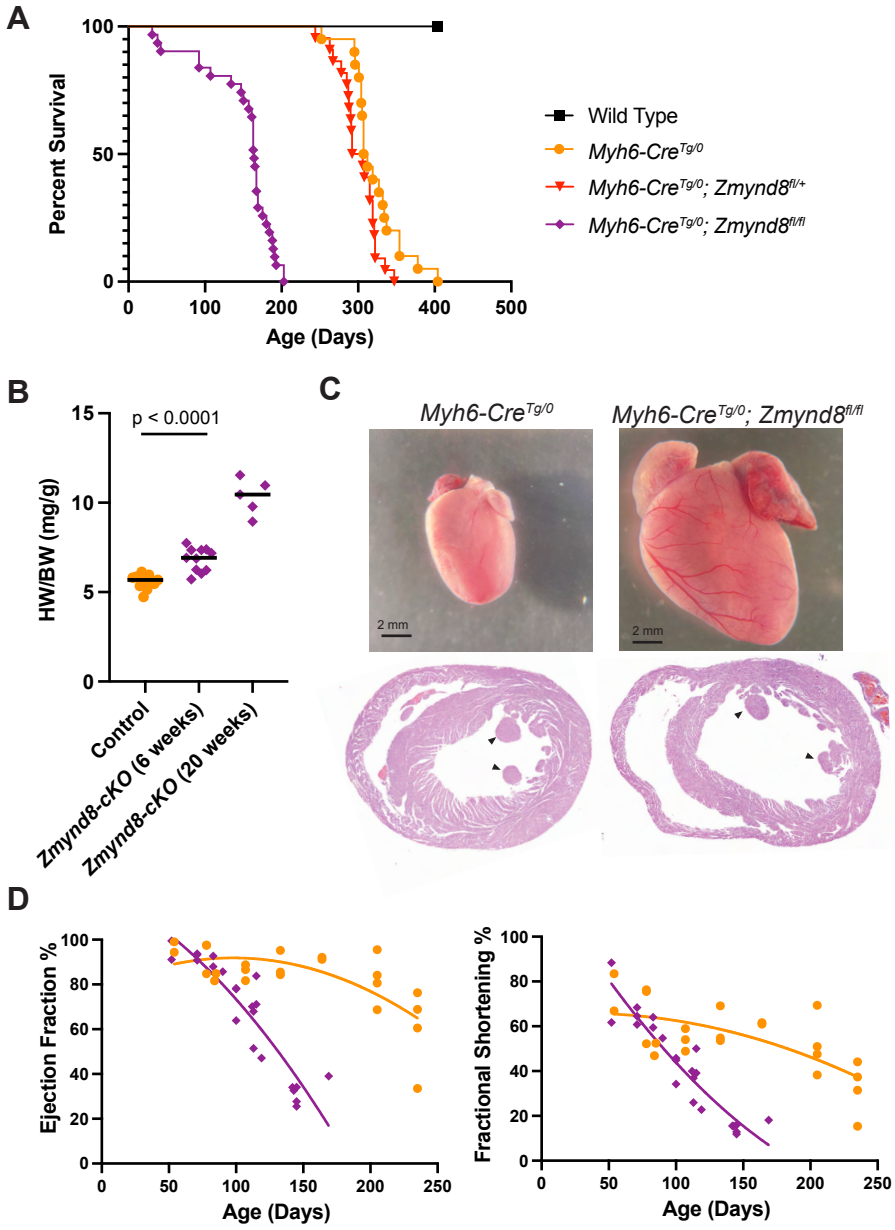
A
Percent Survival
Age (Days)
Wild Type
Myh6-Cre Tg/0
Myh6-Cre Tg/0; Zmynd8 fl/+
Myh6-Cre Tg/0; Zmynd8 fl/fl
B
HW/BW (mg/g)
p < 0.0001
Control
Zmynd8-cKO (6 weeks)
Zmynd8-cKO (20 weeks)
C
Myh6-Cre Tg/0
Myh6-Cre Tg/0; Zmynd8 fl/fl
2 mm
2 mm
D
Ejection Fraction %
Age (Days)
Fractional Shortening %
Age (Days)

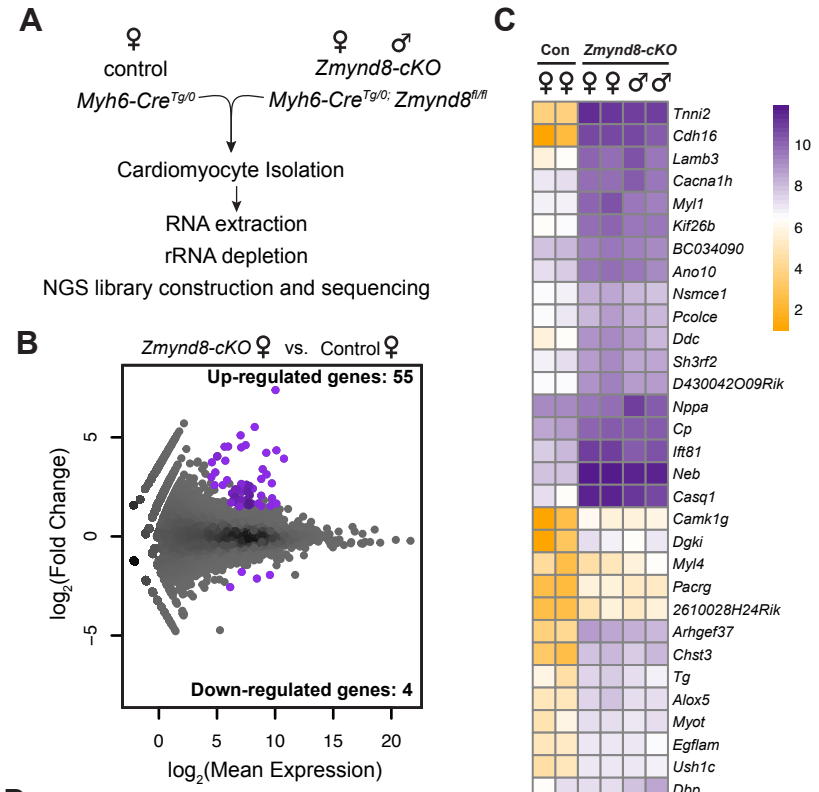

D

GO Term	Benjamini
Striated muscle contraction	5.0E-2
Ion Transport	1.0E-1
Muscle Contraction	2.1E-1
Localization	2.1E-1
Cardiac muscle contraction	3.8E-1
Skeletal muscle contraction	5.5E-1

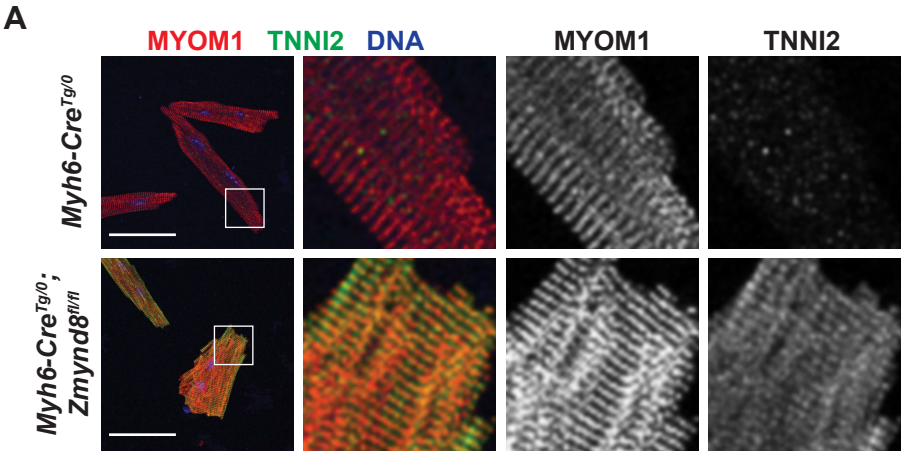
A
MYOM1
TNNI2
DNA
MYOM1
TNNI2
Myh6-Cre Tg/0
Myh6-Cre Tg/0 ; Zmynd8 fl/fl

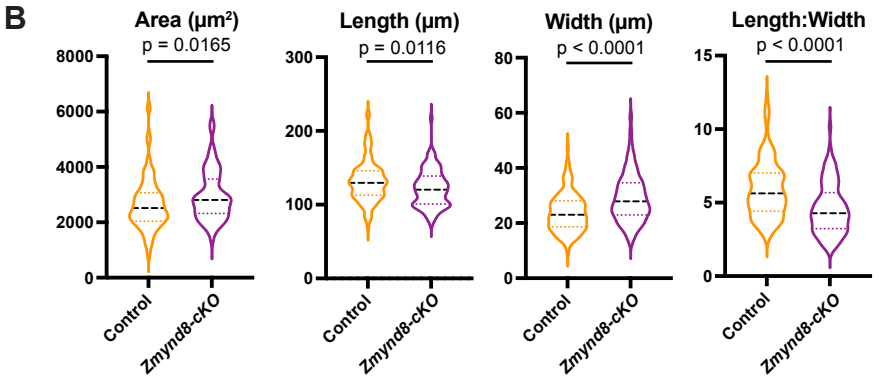
B
Area (μm²)
p = 0.0165
Length (μm)
p = 0.0116
Width (μm)
p < 0.0001
Length:Width
p < 0.0001
Control
Zmynd8-cKO

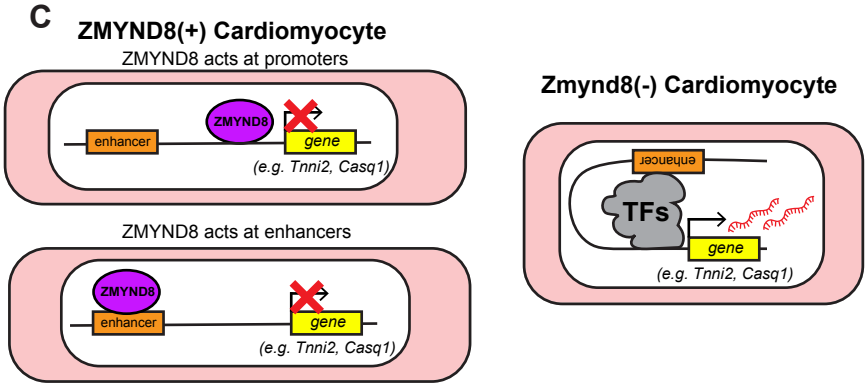
C
ZMYND8(+) Cardiomyocyte
ZMYND8 acts at promoters
ZMYND8
enhancer
gene
(e.g. Tnni2, Casq1)
ZMYND8 acts at enhancers
ZMYND8
enhancer
gene
(e.g. Tnni2, Casq1)
Zmynd8(-) Cardiomyocyte
enhancer
TFs
gene
(e.g. Tnni2, Casq1)

A

Nkx2.5-Cre$^{Tg/0}$*; Zmynd8*$^{fl/+}$ **X** *Zmynd8*$^{fl/fl}$

Genotype	Expected (%)	Observed (%)
Zmynd8$^{+/fl}$	5.75 (25)	7 (30)
Zmynd8$^{fl/fl}$	5.75 (25)	3 (13)
Nkx2.5-Cre$^{Tg/0}$*; Zmynd8*$^{fl/+}$	5.75 (25)	7 (30)
Nkx2.5-Cre$^{Tg/0}$*; Zmynd8*$^{fl/fl}$	5.75 (25)	6 (26)

B

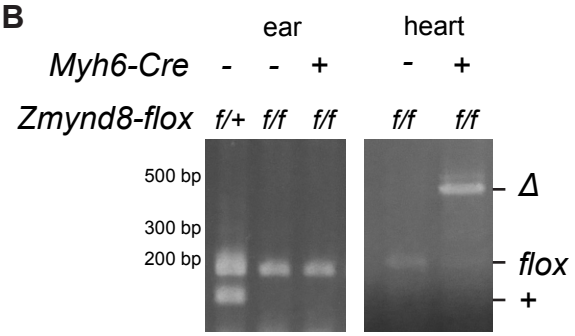

C

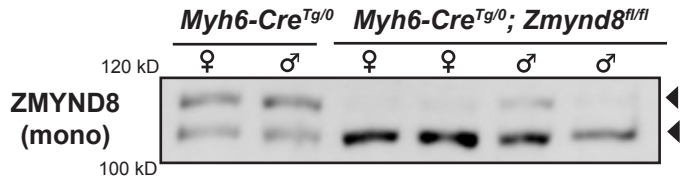

D

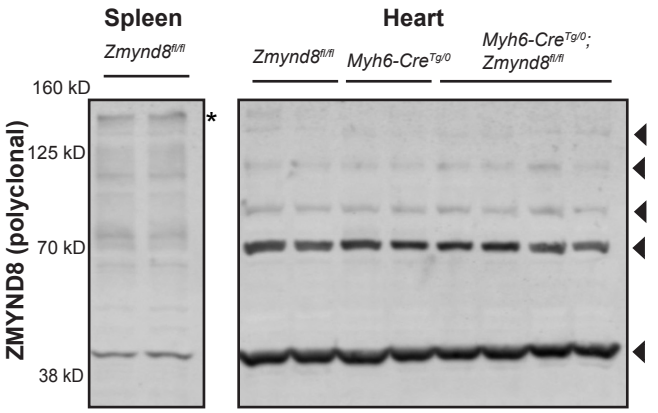

E

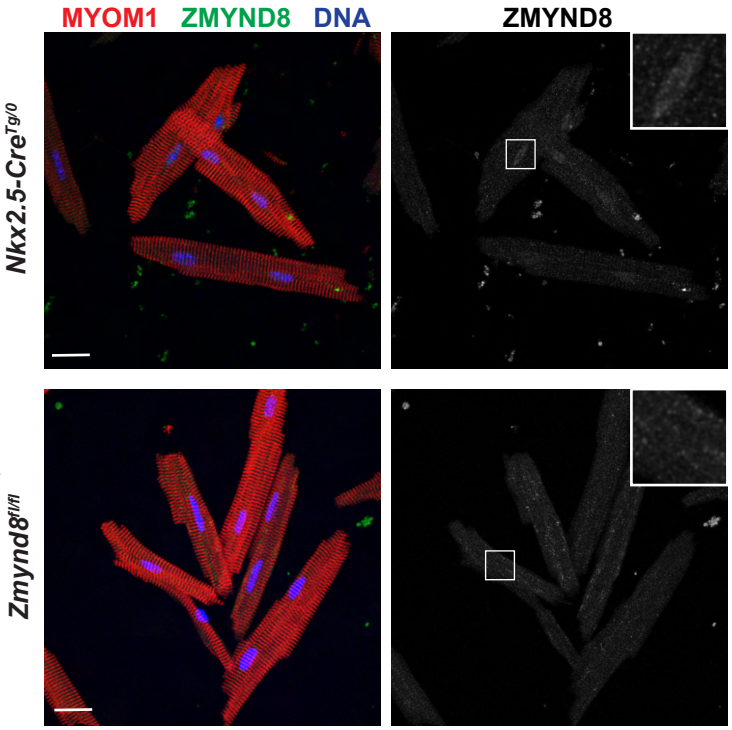

Supplemental Figure 1. Conditional knockout of *Zmynd8* from mouse cardiomyocytes. A) Mendelian ratios of F1 progeny from *Nkx2.5-Cre*$^{Tg/0}$*; Zmynd8*$^{fl/+}$ males mated to *Zmynd8*$^{fl/fl}$ females. B) PCR amplifcation of ear and heart tissue from *Zmynd8*$^{fl/+}$, *Zmynd8*$^{fl/fl}$, and *Myh6-Cre*$^{Tg/0}$*; Zmynd8*$^{fl/fl}$ mice. The delta (*Δ*), flox, and wild type (+) alleles are indicated to the right. C) Immunoblot of heart extracts from *Myh6-Cre*$^{Tg/0}$ and *Myh6-Cre*$^{Tg/0}$*; Zmynd8*$^{fl/fl}$ male and female mice using a monoclonal ZMYND8 antibody. D) Immunoblot of spleen and heart extracts from *Myh6-Cre*$^{Tg/0}$ and *Myh6-Cre*$^{Tg/0}$*; Zmynd8*$^{fl/fl}$ mice using a polyclonal ZMYND8 antibody. Asterisk indicates expected size of full-length ZMYND8. E) Immunofluoresence images of cardiomyocytes isolated from *Nkx2.5-Cre*$^{Tg/0}$ and *Nkx2.5-Cre*$^{Tg/0}$*; Zmynd8*$^{fl/fl}$ mice stained for MYOM1 (red), ZMYND8 (green), and DNA (blue). Boxed nuclei are expanded in the upper right corner. Scale bars are 20 µm.

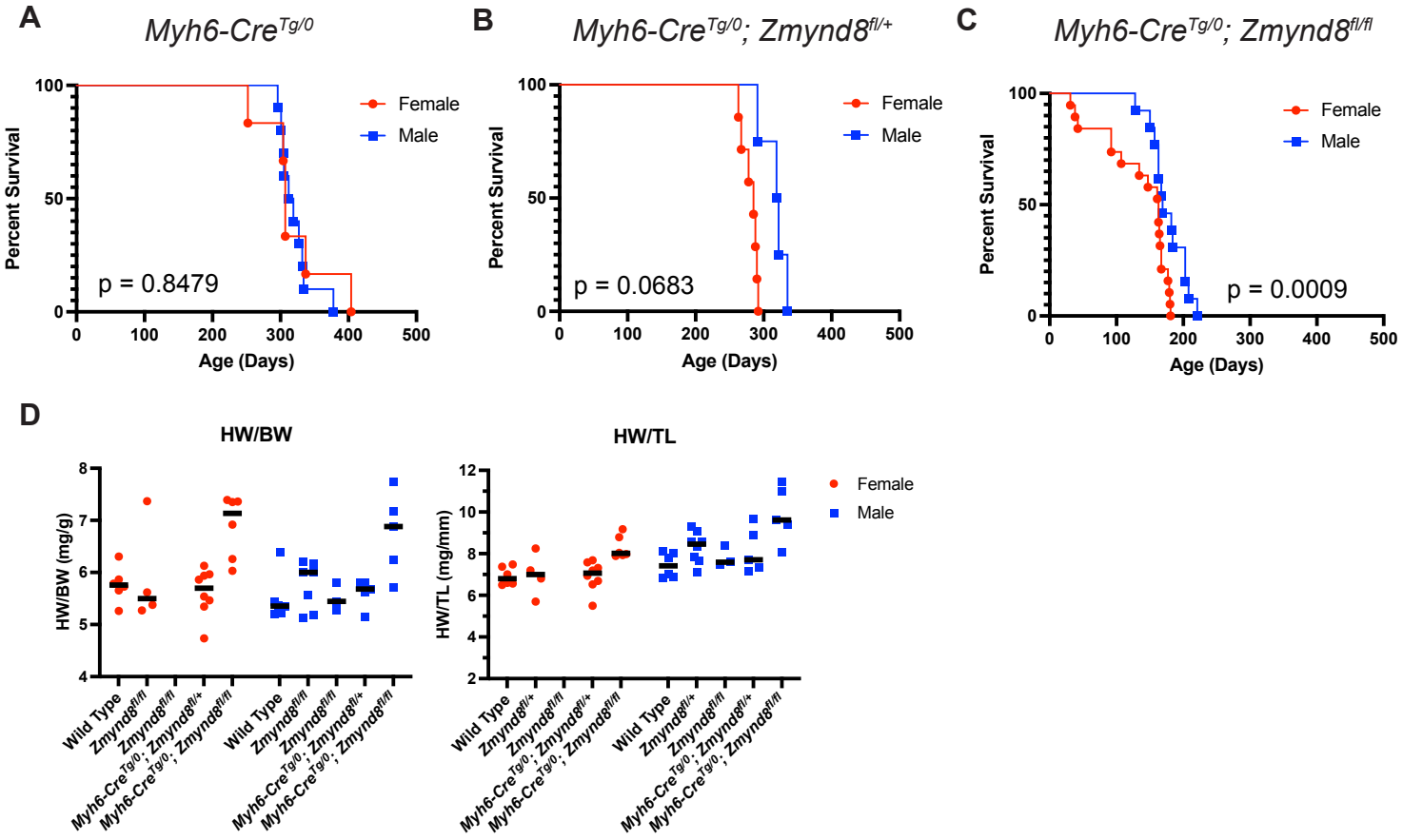

Supplemental Figure 2. Lifespan and heart weight measurements disaggregated by sex **A-C)** Lifespan curves for *Myh6-Cre*$^{Tg/0}$ (A), *Myh6-Cre*$^{Tg/0}$*; Zmynd8*$^{fl/+}$ (B) and *Myh6-Cre*$^{Tg/0}$*; Zmynd8*$^{fl/fl}$ (C) mice separated by females (red circles) and males (blue squares). P-values determined by the log-rank test are indicated for each curve. Lifespan comparison data are found in Supplementary File 1. D) Heart weight to body weight or tibia length measurements of male and female 6-week-old mice.

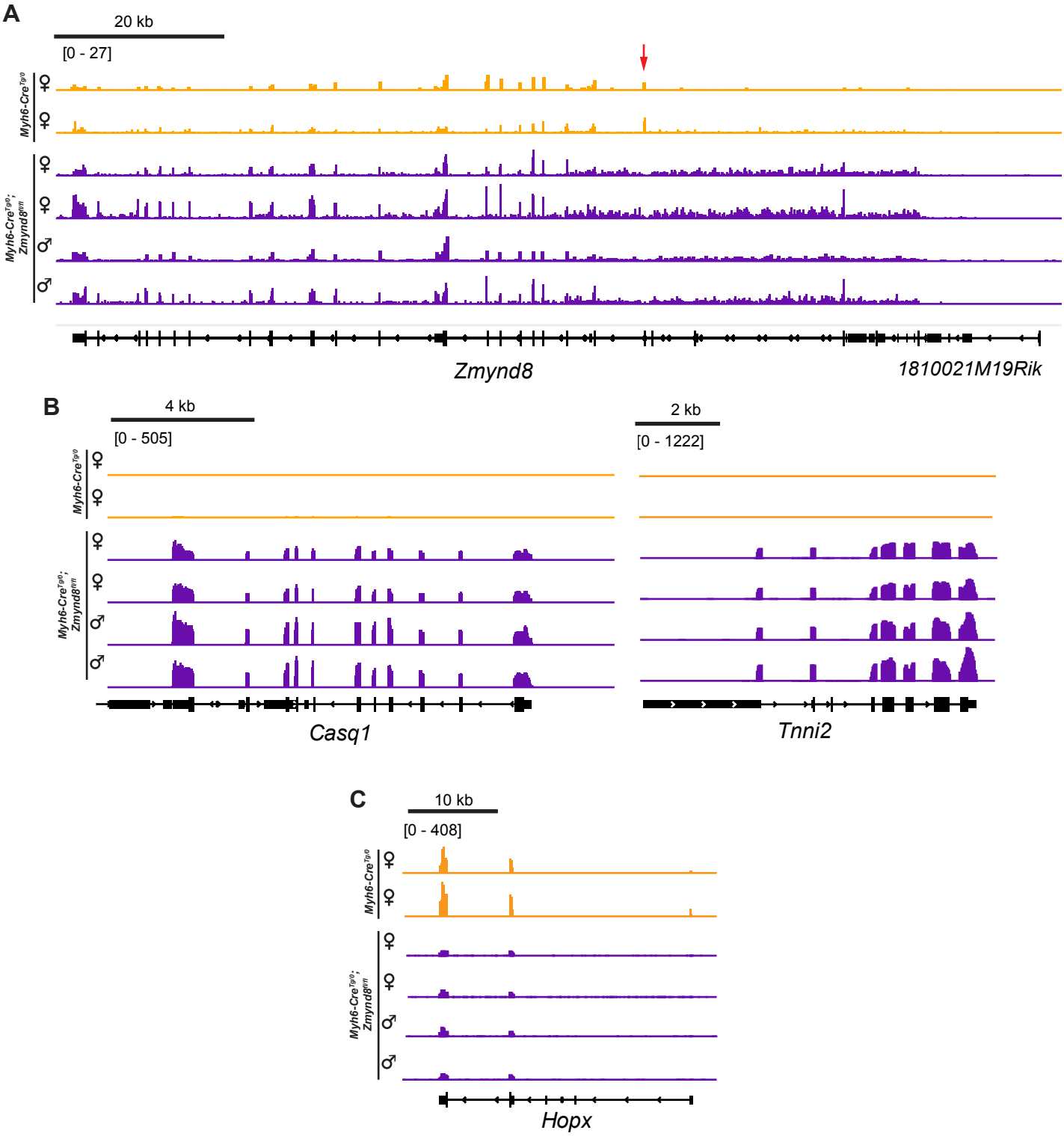

Supplemental Figure 3. IGV genome browser tracks showing reads from *Myh6-Cre*$^{Tg/0}$ control (orange) and *Myh6-Cre*$^{Tg/0}$*; Zmynd8*$^{fl/fl}$ (purple) cardiomyocytes across A) *Zmynd8* with exon 4 indicated (red arrow), B) the skeletal muscle genes *Tnni2* and *Casq1*, and C) the homeodomain factor gene *Hopx*. For each gene, all samples are set to the same scale, indicated in brackets below the scale bar.

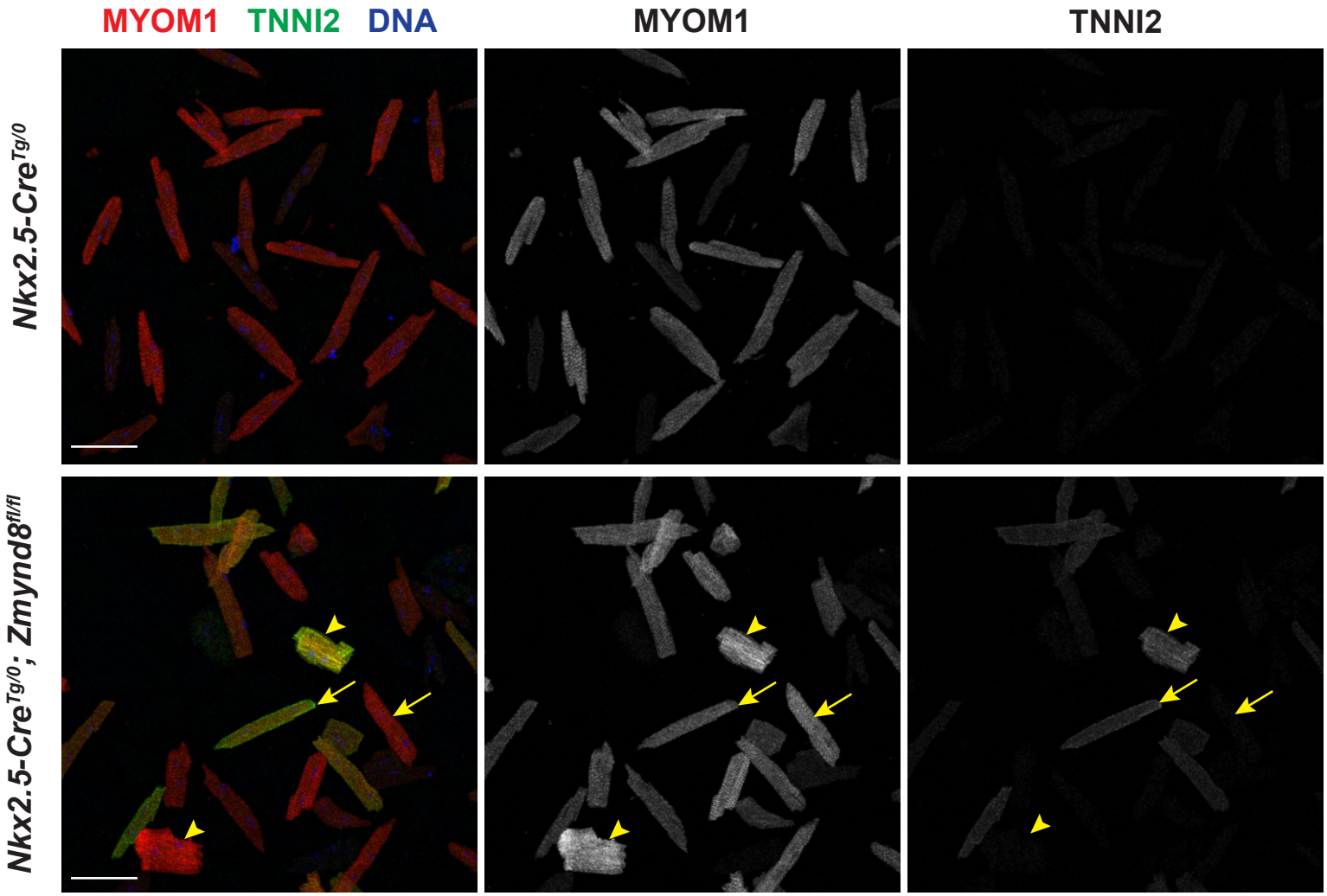

Supplemental Figure 5. Cardiomyocytes from *Nkx2.5-CreTg/0* or *Nkx2.5-CreTg/0; Zmynd8-fl/fl* mice stained for MYOM1 (red), TNNI2 (green), and DAPI (blue). Arrows indicate cardiomyocytes with normal morphology and arrowheads are cardiomyocytes with distorted morphology. Scale bars are 50 µm.